Alpha capture into the giant quadrupole resonance in ^{28}Si

E. Kuhlmann
Institut für Experimentalphysik I, Ruhr-Universität Bochum, D4630 Bochum, Federal Republic of Germany

K. A. Snover, G. Feldman, and M. Hindi
Department of Physics, University of Washington, Seattle, Washington 98195
(Received 8 October 1982)

Angular distributions have been studied in the ^{24}Mg$(\alpha,\gamma_0)^{28}$Si reaction in fine energy steps for excitation energies $14 \lesssim E_x \lesssim 22$ MeV. Absolute cross sections were determined with errors smaller than 10% and were found to be substantially lower than previously determined. A total $E2$ strength of (3.7 ± 0.4)% of the energy weighted sum rule was observed, in good agreement with results obtained from $(\alpha,\alpha'\alpha_0)$ coincidence experiments. Strong interference effects as well as other deviations from statistical model expectations are interpreted as due to nonstatistical preequilibrium effects in both $E1$ and $E2$ channels.

[NUCLEAR REACTIONS ^{24}Mg$(\alpha,\gamma_0)^{28}$Si, $E=4.3-14.0$ MeV; measured $\sigma(E,E_\gamma,\theta_\gamma)$. ^{28}Si deduced $E1$, $E2$ strengths. Enriched target. Compared decay strengths with Hauser-Feshbach estimates, including effects of isospin.]

I. INTRODUCTION

In recent years considerable interest has been focused on the isoscalar giant quadrupole resonance (GQR). Information on light nuclei has mainly been gathered from inelastic alpha-scattering experiments.[1–4] The GQR was found to be fairly broad as well as highly structured; for the even-even nuclei of the lower half of the *sd* shell an average strength of about 30% of the energy weighted sum rule (EWSR) was observed which was distributed over an energy range of up to 10 MeV.[2–4] A question of central interest is to what extent the GQR decays in a direct way to certain final states, thus keeping memory of its original 1p-1h excitation, or whether this memory is lost by mixing with more complex np-nh configurations, which results in a decay approaching the statistical limit. From extensive coincidence experiments[5–8] the main decay branches of the GQR's in several light nuclei were unraveled. By comparing the experimental results with Hauser-Feshbach calculations, a shift from a prevailing direct decay in the very light nuclei (^{16}O, ^{20}Ne, ^{28}Si) to a predominantly statistical decay for the heavier ones (^{40}Ca) was observed.[7] A dominant α decay was reported for the nuclei ^{16}O and ^{20}Ne,[5,7] whereas in ^{40}Ca the decay proceeds mainly through proton channels to high lying states in ^{39}K.[9] An intermediate situation is found in ^{28}Si, where the decay into the proton and alpha channels occurs with about equal branching ratios.[7,8] Neutron decay in all cases is hindered by the rather high n thresholds, and contributes at most 10%. The surprisingly high contribution of the α breakup of the GQR in light nuclei was explained by Hecht and Braunschweig as being due to a strong overlap of the giant $E2$ resonances with α-cluster states with good SU(3) symmetry.[10]

The charged particle capture reactions which worked so well for the investigation of the giant dipole resonance have had only moderate success in the study of the GQR. Although α capture on spin zero target nuclei allows for an easy extraction of the $E2$ strength, this advantage is counterbalanced by the fact that only the ground-state α_0 branch is observable, which in general carries a small fraction of the total strength. In detailed α-capture studies on target nuclei in the mass range $12 \lesssim A \lesssim 28$, on the average 10% of the EWSR was found.[11–13]

Despite this disadvantage, α capture has to be considered a powerful tool in the investigation of the GQR for several reasons:

(i) The $E2$ yield may be observed in the presence of virtually no background since the only other process which is present is the $E1$ decay of the giant dipole resonance (GDR), which can be separated out in a model independent way by means of angular distribution measurements.

(ii) Direct $E2$-capture contributions, which give an underlying continuous background, are known to play a substantial role in the capture of protons and in fact account for all the $E2$ strength observed in the $^{14}C(\vec{p},\gamma)^{15}N$ reaction.[14] In α capture, however, these contributions are small.

(iii) The absolute strength associated with the α_0 channel can be measured with an error as small as 10%, which, together with the results from the analogous $(\alpha,\alpha'\alpha_0)$ coincidence experiments, yields an independent check on the extraction of $E2$ strength from inelastic alpha scattering data.

(iv) The fine structure within the GQR can be investigated with better energy resolution in α capture than in inelastic alpha scattering.

In this paper a detailed study of the GQR in ^{28}Si by means of the $^{24}Mg(\alpha,\gamma)^{28}Si$ capture reaction is described. This reaction has previously been studied with the main emphasis placed on the determination of the $E1$ yield.[15,16] Only a few angular distributions have previously been measured, thus yielding an incomplete picture of the $E2$ resonance. Furthermore, severe doubts exist on the published cross sections,[15] which in the light of other alpha capture experiments[12,13] seem to be too high. According to Ref. 15 the α_0 branch carries as much as 14.5% of the total $E2$ strength, which is in clear disagreement with the reported 4% found in coincidence experiments.[6,8]

Another interesting aspect which prompted the present investigation to be done in fine energy steps was the suggestion that the structures found in inelastic α scattering on ^{28}Si (Refs. 3, 4, and 6–8) did not always line up with the structures found in the $(\alpha,\alpha'\alpha_0)$ coincidence spectra.[6,7] Since the deduced widths of these structures were appreciably broader than the mean coherence widths for pure Ericson fluctuations—in that case shifts in different decay channels were to be expected—it is thought that in ^{28}Si intermediate structure effects play a substantial role.[6] An interpretation in terms of an interference of quasibound cluster states with a broad coherent giant resonance is suggested, which in turn gives a straightforward explanation for the occurrence of uncorrelated yield in the specific (α_0) cluster decay channel. Since, however, a rather trivial reason for the observed shifts would be an interference phenomenon between the α_0-decay amplitude of the GQR and quasifree scattering processes, an independent determination of the fine or intermediate structures associated with the α_0 channel is highly desirable. The coincidence experiments on ^{28}Si showed that the GQR decays by a strong branch into the α_0 channel[6]; thus the study of the inverse α-capture reaction seems most suitable.

Alpha capture into the GDR is believed to proceed predominantly through compound nuclear channels, based on a statistical analysis[16] and calculations in the framework of the Hauser-Feshbach formalism.[12,13] Only a very small fraction ($\approx 1\%$) of the total $E1$ strength is contained in the α_0 channel. Yet, in α capture the γ radiation is mainly of $E1$ character even in self-conjugate nuclei, in which the formation of the GDR is isospin forbidden. The influence of the isospin selection rule is felt in a reduction of the $E1$ cross section, as shown from a comparative study of α capture on self-conjugate nuclei and their respective isotopic, nonconjugate even-even nuclei.[13] These findings are in contradiction to the results reported in Ref. 16 on the reactions $^{24,26}Mg(\alpha,\gamma)^{28,30}Si$, where in fact the isospin forbidden cross section was found to be the larger one. In the present experiment we focus some attention on this issue.

II. EXPERIMENT

The $^{24}Mg(\alpha,\gamma)^{28}Si$ reaction was measured in the energy range $4.3 \leq E_\alpha \leq 13.98$ MeV using metallic, highly enriched ^{24}Mg targets. Alpha particles were produced by the University of Washington FN tandem Van de Graaff accelerator. The capture γ rays were observed in a 25 cm $\varnothing \times 25$ cm NaI (T1) spectrometer with a plastic anticoincidence shield placed at a distance of 37 cm to the target. Typical spectra as obtained at selected bombarding energies are shown in Fig. 1. The excellent resolution of the spectrometer (3.2% at $E_\gamma = 20$ MeV) allowed for an easy extraction of the γ_0 yields by adding the events within a suitable window. The lower ($E_<$) and the upper ($E_>$) limits of the window were defined by $E_< = 0.95E_{\gamma_0}$ and $E_> = 1.04E_{\gamma_0}$, respectively.

The absolute efficiency of the NaI(T1) spectrometer at $E_\gamma = 15$ MeV was measured by taking a thick target yield curve of the $^{12}C(p,\gamma)^{13}N$ resonance reaction at $E_p = 14.23$ MeV. On top of this resonance the thick target (resonance minus background) yield at $\theta = 125°$ is known to be

$$Y_{\text{res}} = (6.66 \pm 0.21) \times 10^{-9}\ \gamma_0\ /\text{proton} .$$

(See Ref. 17.) Analyzing the p-capture spectra in the same way as the spectra obtained in the α-capture experiments, the efficiency was found to be

$$\epsilon\Omega/4\pi = (1.86 \pm 0.08) \times 10^{-3} .$$

With increasing γ-ray energy a 3%/MeV decrease of the efficiency was taken into account.

Special precautions were taken in the handling of the metallic ^{24}Mg targets. Rolled to nominal thicknesses of 0.25, 0.50, and 1.0 mg/cm^2 the targets (manufactured by F. G. Karasek, Argonne, Illinois) were shipped in vacuo and mounted onto the target

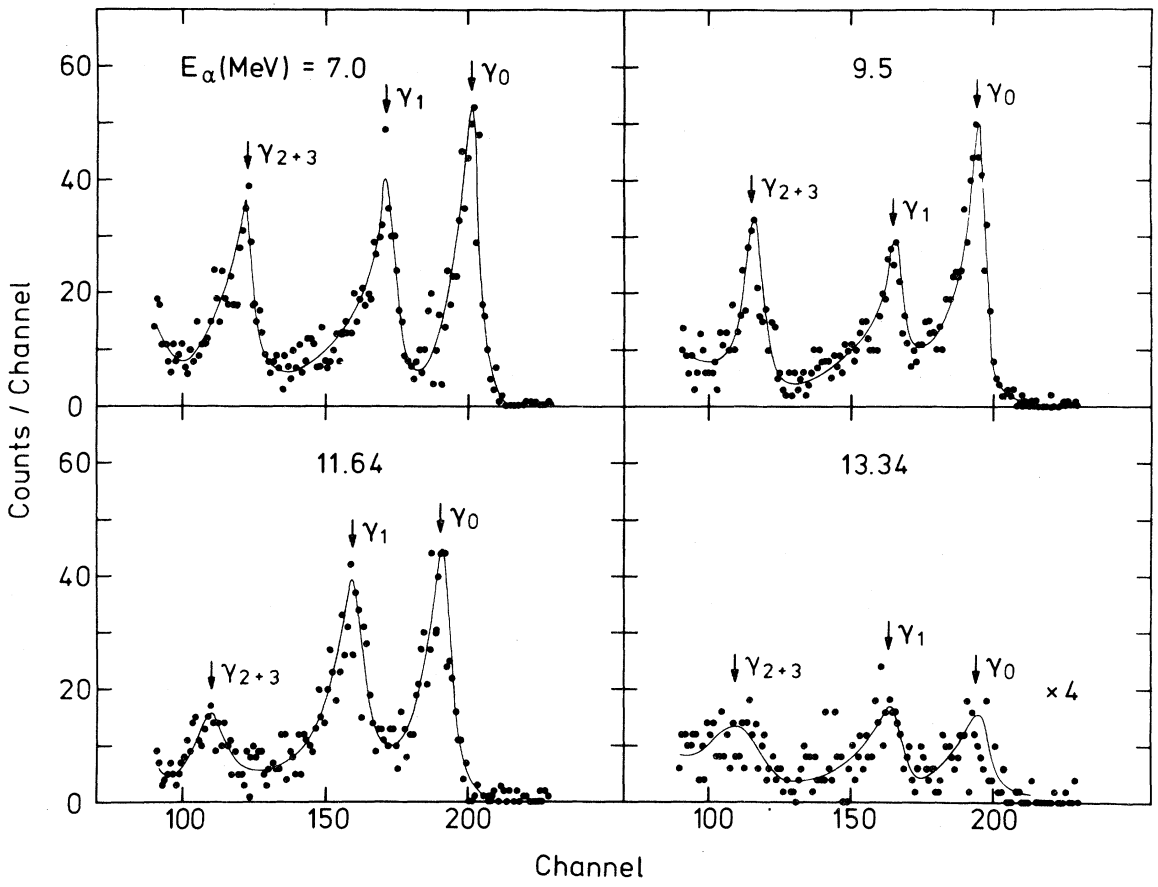

FIG. 1. Sample spectra for the reaction $^{24}Mg(\alpha,\gamma)^{28}Si$ obtained at four different bombarding energies. The solid lines are drawn to guide the eye.

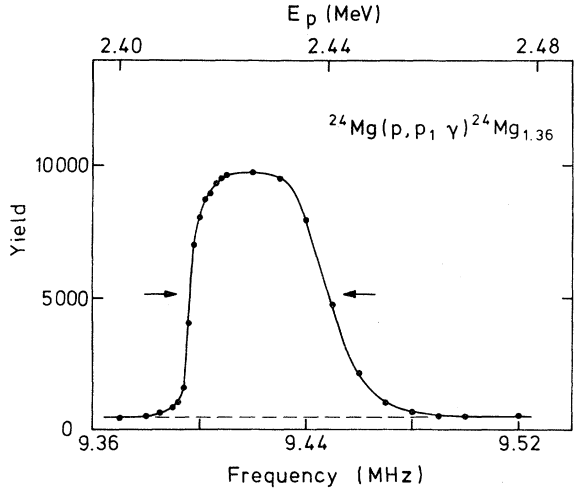

FIG. 2. Resonance yield of the reaction $^{24}Mg(p,p_1\gamma)^{24}Mg_{1.36}$ around a narrow resonance at $E_p=2.42$ MeV as obtained in determination of target thicknesses. The extracted half-thickness of $t=52$ kHz corresponds to an energy loss of $\Delta E=26.5$ keV.

ladder in an Ar atmosphere. The actual target thicknesses were measured by taking excitation functions of the reaction $^{24}Mg(p,p_1\gamma)^{24}Mg_{1.36}$ around a narrow resonance at $E_p=2.42$ MeV. The one obtained with the thinnest target is shown in Fig. 2. A half-thickness of $t=52$ kHz corresponding to an energy loss of 26.5 keV is found. From these measurements and stopping power data as given in Ref. 18 total thicknesses of 267, 556, and 1250 $\mu g/cm^2$ were found, each with an estimated error of about $\pm 5\%$. The individual targets were used for bombarding energies 4.3—7.0, 7.25—12.0, and 12.34—13.98 MeV, respectively. Data were taken in E_α step sizes equal to the target thickness, which ranged from 150 keV at the lowest to 340 keV at the highest energy. Thus a total of 48 five-point angular distributions were taken with the detector set at 45°, 60°, 90°, 115°, and 135°. A 12.7 cm $\varnothing \times 15.2$ cm NaI(T1) crystal at $d=14$ cm was used as a monitor detector during these runs.

The oxygen content of the targets was determined

by making use of the cross section for the reaction $^{16}O(\alpha,\alpha_1\gamma)^{16}O_{6.13}$ (Ref. 19) and found to be smaller than 2%. Employing a Ge(Li) detector at 90° spectra were taken around $E_\alpha = 12$ MeV, where the cross section for the above reaction shows a maximum of about 40 mb/sr. The absolute efficiency of the Ge(Li) detector at $E_\gamma = 6.1$ MeV was measured by use of a calibrated Pu-^{13}C source.

III. RESULTS

The ground state angular distributions were fitted by the expression

$$W(\theta)=\frac{1}{4\pi}\{(\sigma_{E1}+\sigma_{E2})-(\sigma_{E1}-0.71\sigma_{E2})Q_2P_2-1.71\sigma_{E2}Q_4P_4-2.68(\sigma_{E1}\sigma_{E2})^{1/2}\cos\delta(Q_1P_1-Q_3P_3)\}\ . \quad (1)$$

The factors σ_{E1} and σ_{E2} are the total cross sections for $E1$ and $E2$ capture, respectively, and δ is the phase difference $(\Phi_1-\Phi_2)$ of the p-wave $E1$ and d-wave $E2$ capture amplitudes. The P_k are Legendre polynomials and the Q_k are attenuation coefficients. This expression implicitly accounts for the fact that the yield vanishes at 0° and 180°. A plot of the extracted cross sections along with $\cos\delta$ is given in Fig. 3 for the entire energy range scanned in the present experiment. The quantities which were varied independently in fitting the angular distributions were σ_{E1}, σ_{E2}, and

$$I \equiv 2.68(\sigma_{E1}\cdot\sigma_{E2})^{1/2}\cos\delta\ ,$$

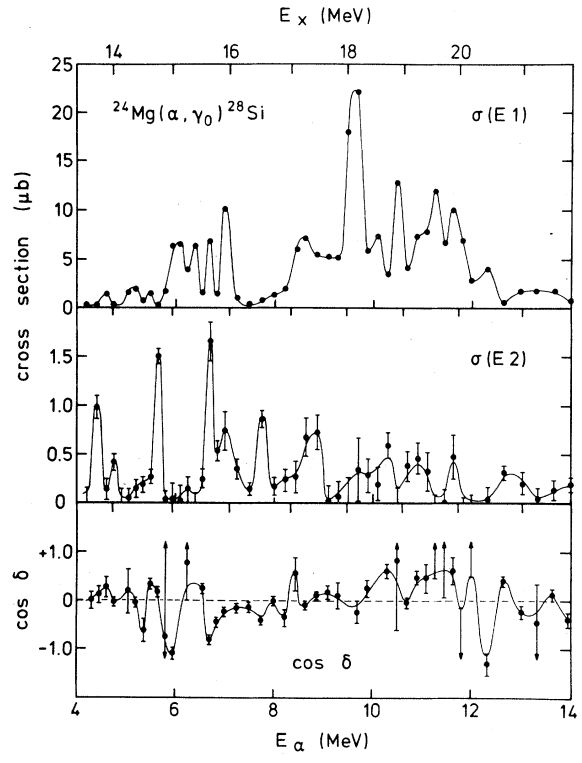

FIG. 3. Extracted total $E1$ and $E2$ cross sections as well as $\cos\delta$ for $^{24}Mg(\alpha,\gamma_0)^{28}Si$.

where I is the coefficient of the $E1$-$E2$ interference term. This ensures that energy averaging, which may affect the extracted values of $\cos\delta$, will not cause inaccuracies in the extracted values of σ_{E1} and σ_{E2}. At several energies the fitted values for σ_{E2} were zero or negative (within 1σ of zero) while I was nonzero. In these cases limits were obtained for $\cos\delta$ shown in Fig. 3 by assuming the 2 standard deviation upper limit for σ_{E2}.

On the average the $E1$ yield amounts to 5 μb with peak cross sections larger than 20 μb. The $E2$ cross section is considerably smaller, and except for three resonances at low excitation energies remains below 1 μb. A lot of structure in the $E1$ as well as the $E2$ yield is observed. The minima in the $E2$ excitation function are always close to zero, which also holds for the $E1$ curve with possibly the exception of a 4 MeV wide interval around 19 MeV. The $E1$ structure is known from an autocorrelation analysis of higher resolution data[16] to have a strong ($\Gamma \approx 65$ keV) "compound nucleus" component and perhaps also a weaker ($\Gamma \approx 300$ keV) intermediate structure component. Our $E2$ results show strong variations with energy indicating semi-isolated resonances (or intermediate structure). At lower energies sharp structure is apparent with width

$$\Gamma \leq \Delta E\ (\text{target}) \approx 130\ \text{keV}\ ,$$

while at higher energies most of the structure is broader. The fact that $\cos\delta$ shows strong deviations from zero indicates that substantial phase information remains in both the $E1$ and $E2$ channels averaged over the target thickness. Hence neither channel can be dominated by fluctuations arising from very narrow overlapping resonances.

Converting the extracted $E1$ and $E2$ cross sections of the α-capture process into those of the inverse (γ,α_0) process by using the principle of detailed balance (Fig. 4), one can compare the observed yields with the respective sum rule limits. The commonly employed sum rules are

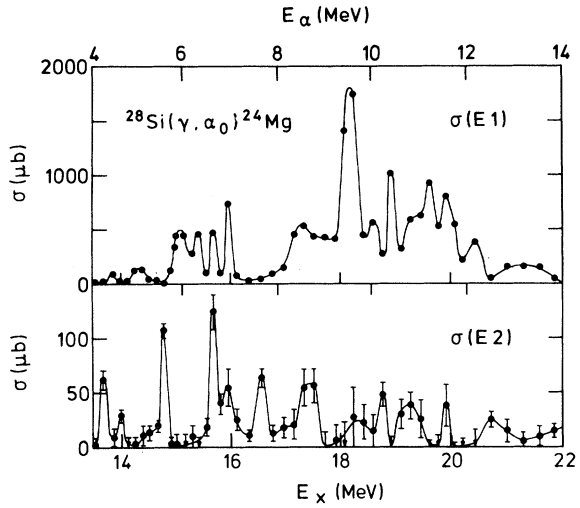

FIG. 4. Total $E1$ and $E2$ cross sections converted by detailed balance to those of the inverse reaction ^{28}Si$(\gamma,\alpha_0)^{24}$Mg.

$$S(E1)=60NZ/A \text{ MeV mb}$$

and

$$S(E2)=0.255Z^2A^{-1}\langle R^2\rangle \mu\text{b/MeV} .$$

In the energy range 13.4–22.0 MeV only a very small fraction of the total $E1$ strength, (0.72±0.05) %, is associated with the α_0 channel. In the same channel and the same energy region, however, considerably more $E2$ strength is found, (3.7±0.4) % of the corresponding sum rule using $\langle R^2\rangle=9.61$ fm^2.

A comparison with previously published values is given in Table I. The dipole cross section as shown in Fig. 4 can be compared directly with the absolute cross section measurements by Meyer-Schützmeister *et al.*[16] Considering the fact that for the present measurements thicker targets were used, the agreement in the observed structures is good. A strong disagreement, however, is found in the magnitude of the extracted cross sections, as can be seen from the integrated total $E1$ strengths (Table I). In Ref. 15 a total yield of 1.2% of the EWSR is given for the energy range 14.5–21.5 MeV, whereas from the present studies in the same energy region only (0.70±0.05) % are observed. The differences are greater in the comparison of the deduced $E2$ yields. According to a reanalysis of the α-capture data presented in Ref. 16, Meyer-Schützmeister *et al.* find 12.2% (Ref. 20) of the total $E2$ strength in a 7 MeV wide interval.[15] This is much more than the presently extracted 3.4% for the same energy region. Furthermore, a concentration of $E2$ strength close to the predicted center of the GQR at $60A^{-1/3}$ MeV is reported in Ref. 15, in disagreement with the present studies (Fig. 4). Reviewing our analysis of the absolute cross section measurements and making a careful check for possible anisotropies in the experimental setup used in the angular distribution studies, we did not find any source of significant systematic errors in the present work. Our confidence in the present results is supported by the number of energies at which a value of zero for σ_{E2} (within errors) was extracted. The Argonne spectra, taken with poorer energy resolution and no cosmic ray suppression,[16] would have been much harder to use to obtain γ_0 yields with a systematic uncertainty of less than several percent. Such precision is necessary for the reliable extraction of $E2$ cross section which is of the order of 10% (or less) of the $E1$ cross section.

Much better agreement, however, is found when comparing the present data with the results of coincidence experiments.[6–8] In Fig. 5 the top part shows the distribution of $E2$ strength $\sigma_{E2}(\gamma,\alpha_0)/E^2$

TABLE I. Percent of $E1$ and $E2$ EWSR observed in ^{28}Si(γ,α_0) and ^{28}Si$(\alpha,\alpha'\alpha_0)$.

Energy interval (MeV)	$\int\sigma_{E1}dE$ (%)		$\int\sigma_{E2}dE/E^2$ (%)		$\int E\cdot\sigma(\alpha,\alpha'\alpha_0)dE$ (%)
	present work	Ref. 15	present work	Ref. 15	Refs. 2 and 8
13.4–22.0	0.72±0.05		3.7±0.4		
14.5–21.5	0.70±0.05	1.2	3.3±0.4	12.2	
15.4–24.8					3.7±0.9[a]
14.1–17.9			2.4±0.3		2.5[a]
17.9–22.0			1.0±0.1		1.7[a]

[a]Calculated from the $E_\alpha=155$ MeV, $\theta_{\alpha'}=6.5°$, $\theta_{\alpha_0}=\theta_R+180°$ spectrum (Ref. 8), assuming a total (α,α') $E2$ strength (Ref. 2) of (34±6) % and an α_0 branching ratio (Ref. 8) of 0.11±0.02 for $E=15.4$–24.8 MeV.

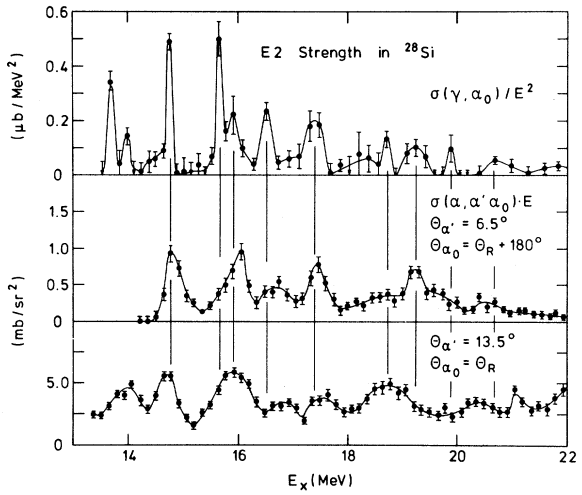

FIG. 5. Top: total $E2$ cross section of the reaction ^{28}Si$(\gamma,\alpha_0)^{24}$Mg weighted by $1/E^2$. Middle: antirecoil coincidence spectrum of the reaction ^{28}Si$(\alpha,\alpha'\alpha_0)^{24}$Mg weighted by E; the inelastically scattered α particles were detected at $\theta_{\alpha'}=6.5°$, the decay α particles at $\theta_\alpha=\theta_R+180°$, where θ_R is the recoil direction (Ref. 8). Bottom: Recoil coincidence spectrum of the reaction ^{28}Si$(\alpha,\alpha'\alpha_0)^{24}$Mg weighted by E; the inelastically scattered α particles were detected at $\theta_{\alpha'}=13.5°$, the decay α particles at $\theta_\alpha=\theta_R$ (Ref. 6).

as deduced from the capture experiment. The $E2$ energy weighted sum rule may be expressed equivalently in terms of

$$\int \sigma_{E2}(\gamma,x)dE/E^2$$

and $\sum E\cdot B(E2)$. Making the approximation in the inelastic α scattering that the sum rule fraction $E\cdot B(E2)$ contained in an interval ΔE at energy E is proportional to

$$E\,d^3\sigma_L(\alpha,\alpha'\alpha_0)/d\Omega_{\alpha'}d\Omega_\alpha dE\ ,$$

one obtains the middle plot in Fig. 5 which shows the antirecoil ($\theta_{\alpha_0}=\theta_R+180°$) coincidence spectrum, normalized to an overall strength[2,8] of $(3.7\pm0.9)\%$ of the EWSR for $E=15.4$–24.8 MeV. The bottom curve shows a similar plot for $\theta_{\alpha_0}=\theta_R$ (with an arbitrary vertical scale.) Both the middle and the bottom curves have been proven by extensive angular distribution studies to reflect predominantly isoscalar $E2$ strength with only minor contributions from other multipolarities.[6,21] The existence of a large amount of structure is apparent in both coincidence spectra. The similarity in shape of the capture data and the antirecoil spectrum as indicated by the vertical lines is impressive. In the bottom curve some underlying continuous background not only tends to dampen the structures but also causes appreciable shifts. Quasifree scattering (QFS) processes are most likely responsible for this background[6,7]; they are known to show their strongest contributions along the recoil direction. In the absence of QFS the structures not only are more pronounced (middle spectrum), but also are closely correlated with the ones deduced from the capture reaction.

The decay experiments yielded an α_0 branching ratio of 0.11 ± 0.02 for $E=15.4$–24.8 MeV.[6,8] Together with a reported total $E2$ strength of $(34\pm6)\%$ this leaves $(3.7\pm0.9)\%$ to be associated with the α_0 channel. For the same energy range $E=14.1$ to 22.0 MeV we find an $E2$ strength of $(3.4\pm0.3)\%$ in (γ,α_0), in reasonably good agreement with $(4.2\pm1.0)\%$ found in $(\alpha,\alpha'\alpha_0)$ (Table I). This confirms the accuracy of the inelastic scattering technique for extracting $E2$ strength, at least in this case. It is worthwhile noting that in the one other case where a similar comparison may be made,[22] namely ^{16}O(γ,α_0) (Ref. 11) and ^{16}O$(\alpha,\alpha'\alpha_0)$ (Ref. 5), $E2$ strengths show similar shapes but quite different magnitudes.

IV. DISCUSSION

A. Decay modes

A study of the decay modes of the GQR may provide important insight into the structure of this resonance, as several coincidence studies have shown.[6–8,21] The question to what extent the various open decay channels (Fig. 6) contribute to the total width is a very intriguing one, and apparently for the light nuclei a direct decay into some selected channels is more favorable than a statistical decay.[7,8] Shown in Fig. 6 are energy and Q-value diagrams for four isobaric systems with $A=16$, 20, 24, and 28. The shaded area indicates the region of the reported GQR, the arrows mark the predicted center $60A^{-1/3}$ MeV. For all systems the α channel opens first; however, due to the strongly increasing Coulomb barrier—given by the dashed line—already in the $A=28$ system the effective p threshold is lower. Several α-decay branches are given,[6] however, no systematic effect is observable. The n channel, which is not blocked by the Coulomb repulsion, in all cases opens roughly one MeV above the effective p threshold (including Coulomb barrier effects), yet contributions into these decay channels do not play a substantial role. On the average they yield less than 10% of the total decay.[6] In a naive picture this is easily understood by use of the Hauser-Feshbach (HF) formalism. Assuming that the decay into each open channel proceeds with its statistical weight given by the magnitude of the corresponding transmission coefficient, the decay mode can be cal-

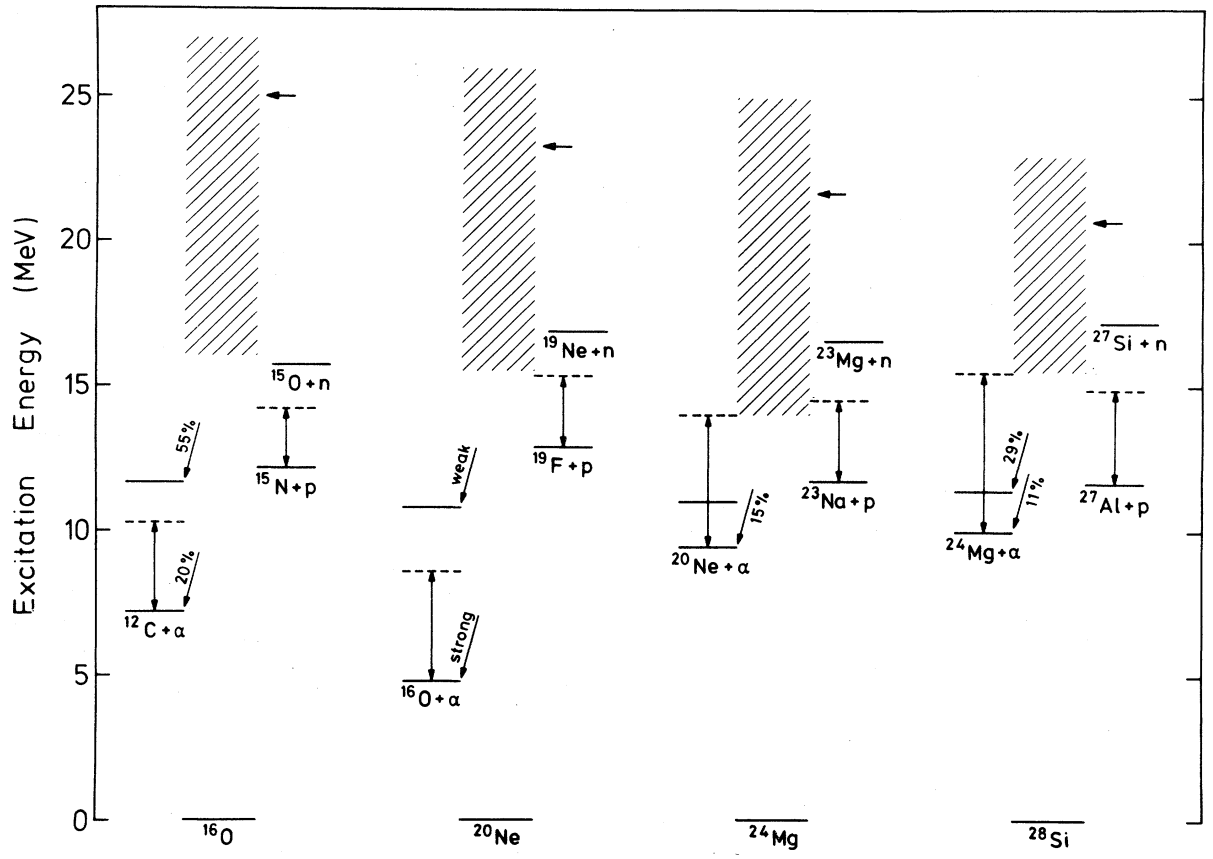

FIG. 6. Energy and Q-value diagrams for four isobaric systems with $A=16, 20, 24, 28$. The α-decay branches (given in %) are from Ref. 6 (see text).

culated. Using the computer code STAT—2 (Ref. 23) and appropriate optical model parameters,[24,25] branching ratios as shown in Fig. 7 are obtained for the (statistical) decay of the GQR in ^{28}Si. Except for the p_0- and α_0-decay channels only total branches for the decay into the α, p, and n channels are given. Significant α_0 decay is found in the energy region below 20 MeV, in agreement with the experimental findings. Alpha decay into higher excited states in ^{24}Mg around 16 MeV almost gets as important as the p decay, which throughout the energy region studied is the dominant channel.

It should be mentioned that for energies just above their respective particle thresholds the relative weight of individual decay channels as predicted from HF cannot be taken too seriously, due to uncertainties in the optical model parameters. Substituting, for instance, the presently used ($\alpha+^{24}$Mg) optical model parameters[25] with those proposed in Ref. 26 but leaving the p and n parameters unchanged will reduce the maximum in the p_0 branching ratio from 0.89 (Fig. 7) to 0.56. Correspondingly the second maximum in the α_0 ratio is shifted towards lower excitation energies, eventually filling out the minimum in between. For energies several MeV above each particular threshold, however, the calculated branching ratios are less sensitive to various sets of optical model parameters.

Comparing the present α-capture data with the

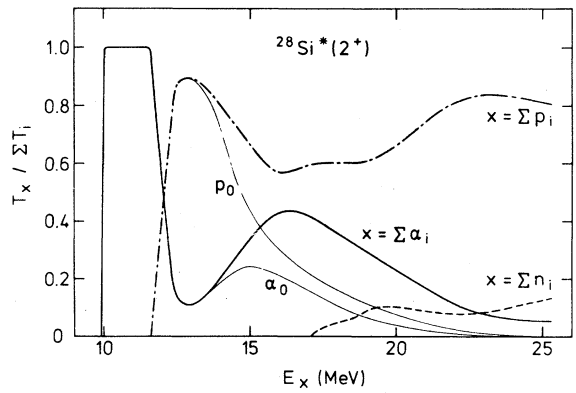

FIG. 7. Energy dependence of branching ratios for various α-, p-, and n-decay channels from $J^\pi=2^+$ states as calculated by a statistical model.

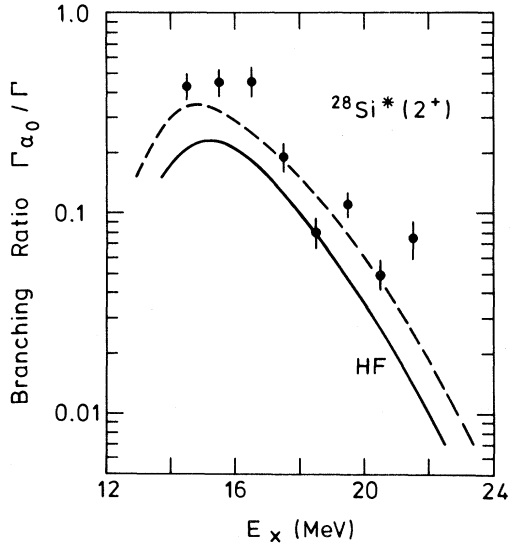

FIG. 8. Energy dependence of the $E2$ α_0 branching ratio obtained from a comparison of the present capture data with the total $E2$ distribution (Ref. 4). The solid line gives the conventional Hauser-Feshbach prediction, which neglects isospin and is valid in the case of complete isospin mixing; the dashed curve results from a modified HF calculation assuming pure isospin (see text).

distribution of $E2$ strength as found in inelastic α scattering,[3,4] experimental branching ratios for the α_0 decay channel as a function of energy are obtained (Fig. 8). The strength distribution reported in Ref. 3 is based on the assumption of a uniform mass distribution. A more realistic Fermi-mass distribution was used in Ref. 4; hence those results were considered in the present calculations. The $E2$-strength distributions as deduced from α capture and (α,α') scattering data and expressed as a percentage of the relevant sum rule limits first were converted into two histograms with 1 MeV wide energy bins. Ratios of the yields of corresponding intervals were then formed, which are given as solid points in Fig. 8. From an almost constant value of roughly 40% around 15 MeV the branching ratio drops below 10% for energies higher than 20 MeV. For the whole energy region studied, the experimental branch is larger than the one predicted from a conventional HF calculation as described above (solid curve). This calculation neglects isospin, and would be correct if isospin is completely mixed in $J^\pi=2^+$ compound states in this energy region. The other extreme of pure isospin in the compound nucleus is given by the dashed curve, which is based on an α-branching ratio given by[27,28]

$$B_\alpha=\frac{T_\alpha}{\sum\frac{1}{2}(T_p+T_n)+\sum T_\alpha},$$

where the factor $\frac{1}{2}$ in the denominator is the square of an isospin Clebsch-Gordan coefficient. This latter curve is in better agreement with the experimental data, although a slight enhancement in the low energy data remains.

This effect of isospin in statistical decay estimates apparently has been neglected in previous discussions of GQR decay branching ratios (see, for example, Refs. 6 and 7). The degree of compound nuclear isospin mixing is not known in the present case, and hence we regard the two curves in Fig. 8 as illustrating a range of possible values. Furthermore, the calculated values shown in Fig. 8 are appropriate only for a resonance with a negligible escape width. If the total escape width $\Gamma^\uparrow$ is appreciable, then the branching ratio for a channel which decays statistically is given by the HF branching ratio multiplied by $\Gamma^\downarrow/\Gamma$, where $\Gamma^\downarrow$ is the spreading width and Γ is the total width ($\Gamma=\Gamma^\uparrow+\Gamma^\downarrow$). The factor $\Gamma^\downarrow/\Gamma$ is just the fraction of the *total* decay strength which is statistical. This fraction (unknown for the GQR) is ≤ 1; hence, there may still be a nonstatistical enhancement of α_0 GQR decays even if compound nuclear isospin is pure.

Such an enhancement is not likely due to a direct $E2$ component; indeed the number of σ_{E2} data points in Fig. 3, which are zero (within errors) indicates that any slowly varying direct component is small. It could arise from the particular doorway configurations which form the dominant part of the GQR in an $A=4n$ nucleus like ^{28}Si. As has been shown in Ref. 10, where group theoretical methods were used in the description of collective features, the giant $E2$ resonances in these nuclei have a large overlap with α-cluster configuration of good SU(3) symmetry. Hence the GQR may have a significant α-decay width arising from an early stage in the np-nh hierarchy. As a result an enhancement over the HF prediction may be expected.

These conclusions can be elaborated on by making similar comparisons of reactions used in the investigation of the GDR in ^{28}Si. High resolution α (Ref. 16) and p-capture[29] studies revealed a highly structured GDR. A statistical analysis of the α-capture data showed that about $(80\pm20)\%$ of the ^{24}Mg(α,γ_0) total $E1$ cross section arises from reactions via the compound nucleus, while the proton capture proceeds predominantly through doorway (nonstatistical) processes.[16,29] Branching ratios for these selected p_0 and α_0 decay channels are deduced by comparing the p- and α-capture data of Ref. 29 and the present investigation, respectively, with the γ-absorption measurements of Ahrens *et al.*[30] As one might expect, two strikingly different plots are obtained (Fig. 9). Very small GDR α_0 branching ratios of $\leq 4\%$ are found which for energies higher

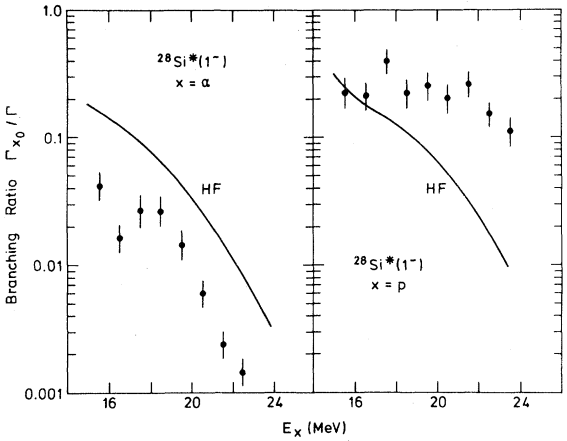

FIG. 9. Energy dependence of the $E1$ α_0 (left) and p_0 branching ratios (right) obtained from a comparison of capture data with γ-absorption measurements (Ref. 30). The α-capture data stem from the present study; the p_0 cross sections are taken from Ref. 29. The solid lines give the Hauser-Feshbach predictions.

than 19 MeV decrease rapidly, in agreement with the energy dependence of HF calculations. This does not mean that α_0 GDR decays are statistical—they may also be enhanced and follow the HF energy dependence as perhaps do the α_0 GQR decays. The absolute magnitude of the HF branching ratio (calculated neglecting isospin) is larger than the data by an almost constant hindrance factor of 4 (see also the following subsection). The experimental p_0 branching ratios show a significant deviation from HF: For excitation energies up to 22 MeV the branching ratio remains almost constant around 25%, whereas in the same energy region the HF calculations predict a decrease by a factor of 10. Clearly, a noncompound reaction mechanism prevails in the p-capture data, as was known previously. In subsection IV D we discuss evidence from an analysis of the $E1$-$E2$ interference factor for substantial nonstatistical components in both the $E1$ and $E2$ α_0 channels.

B. Isospin mixing in the GDR

The observed hindrance for α capture into the GDR (Fig. 9) relative to the HF predictions may be attributed to the isospin selection rule (assuming this channel to be predominantly statistical), since isospin has been neglected in the present HF calculations. A comparable reduction by a factor of 4 for isospin forbidden (compound) reactions was also found in a previous analysis of α-capture reactions.[31] Hence we conclude that in the excitation of the GDR by means of the reaction ^{24}Mg(α,γ)^{28}Si, isospin plays an important role. Much stronger isospin mixing, as reported in Ref. 16, is in disagreement with the present study. In this context it would be worthwhile to check the absolute cross sections of the reaction ^{26}Mg(α,γ)^{30}Si. The conclusion of strong mixing[16] was mainly derived from the observation that for this reaction significantly smaller cross sections were found than for ^{24}Mg(α,γ)^{28}Si. A comparison of ^{24}Mg(α,γ)^{28}Si cross sections from Ref. 16 with the present results (Table I) indicates that the former data are too high by about 40%.

C. Structure in the GQR

The GQR primarily is understood as a $2\hbar\omega$ 1p-1h excitation. Its signature is reflected in a fairly broad and unstructured resonance. The coupling of this primary doorway to more complicated levels such as 2p-2h (secondary doorways or hallways), 3p-3h,. . ., np-nh states, however, may lead to more structure. From a theoretical point of view only the two extremes, the primary doorway at the beginning and the compound nucleus at the end of the np-nh hierarchy, are reasonably well understood and detailed calculations for many nuclei are available. Explicit inclusion of 2p-2h or 3p-3h components have been tried in a few instances with limited success. Direct-semidirect (doorway) reaction models have been developed in the description of proton capture studies in light nuclei with the result that most of the $E2$ strength observed is attributed to direct capture.[14] From an experimental point of view one might try to distinguish gross (the primary doorway) and fine structure (the compound nucleus) as well as intermediate structure (2p-2h, 4p-4h, or anything before reaching the final stage of the compound nucleus).

As for ^{28}Si it is known that the fine structure width around $E_x = 19$ MeV is of the order of 65 keV.[16] Since in the present experiment the angular distributions were taken in steps corresponding to the target thickness [which were always larger than 150 keV (Sec. II)], most of the compound nuclear effects have been averaged out. According to Refs. 2–4 and 8, the highly structured GQR in ^{28}Si is centered near 19 MeV and has a gross width of 5–6 MeV. The $E2$ distribution as observed in the present capture experiment (Figs. 4 and 5) does not reflect a broad resonance, but many narrower resonances with widths $\lesssim$ 400 keV are found. This is in agreement with the (α,α') and $(\alpha,\alpha'\alpha_0)$ results of Refs. 2 and 8, which suggest that the α_0 $E2$ strength is more fragmented than the total $E2$ strength. On the other hand, the α_0 $E2$ fragmentation we observe is similar to the fragmented total $E2$ strength found by Van der Borg *et al.*[4] in (α,α') studies.

This fragmentation is interpreted as being due to nonstatistical structure effects primarily because the phase factor cosδ shows strong deviations from zero at all energies. Over a wide range at high energies the average value of cosδ is substantially positive (0.3 for $E_x = 18.4$–20.7 MeV). This requires strong nonstatistical components in both the $E1$ and $E2$ channels, as is discussed in more detail in subsection D below. Interference effects in $(\alpha,\alpha'\alpha_0)$ (Ref. 8) provide independent evidence for some nonstatistical contributions in the $E2$ channel. Also there is a suggestion that the α_0 branching ratio (Fig. 8) is underestimated by the HF predictions (subsection IV A), although the energy dependence is similar to that of HF.

The present results do not allow us to distinguish whether the nonstatistical effects in the $E2$ α_0 channel are due to the primary doorway (as is possible according to the work of Ref. 10) or to more complicated preequilibrium effects.

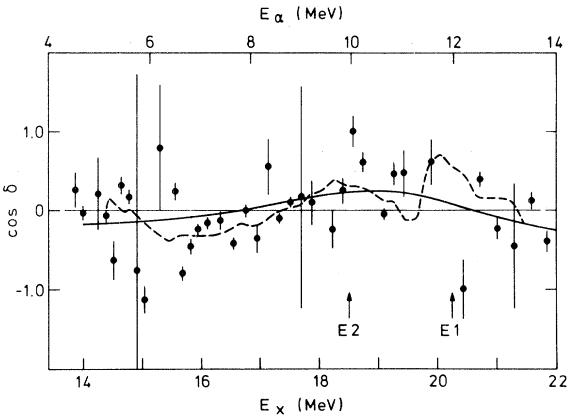

FIG. 10. cosδ vs E_x. Solid points represent the measured data (limit values—see Fig. 3—have been omitted). Dashed curve: smoothed data obtained from quadratic polynomial fitting to the solid points; solid curve: a calculation of interfering GDR and GQR with $E_1 = 20.25$, $\Gamma_1 = 4.5$, $E_2 = 18.5$, and $\Gamma_2 = 6$ MeV.

D. Gross structure in the phase factor cosδ

Figure 3 shows cosδ versus energy, where δ is the relative phase between the interfering $E1$ and $E2$ amplitudes in the ^{24}Mg$(\alpha,\gamma_0)^{28}$Si reaction. Strong, rapid variations are apparent, associated with the narrow (≤ 400 keV) structure in σ_{E1} and σ_{E2}. There is also the strong suggestion of a more slowly varying gross structure in cosδ corresponding to negative values in the region $E_x = 15$–17 MeV, positive values for $E_x = 18$–20 MeV, and zero or slightly negative values at the highest energies.

In order to make these observations more quantitative, we have smoothed the data by doing a polynomial fit to the data points within a window of fixed size stepped along the energy axis. For each step the value of the fitted polynomial at the center of the window is computed and a curve is drawn connecting these central values obtained for different window positions. Figure 10 (dashed curve) shows the results of this procedure for quadratic fits with a window size $\Delta E_x = 2$ MeV and a step size of 0.2 MeV. The shape of this curve provides evidence for the sort of gross structure discussed above. The minimum near 19.5 MeV should not be taken too seriously, as it depends on only one data point. The smoothed gross structure shape is independent of the order of polynomial fitted (2, 3, or 4) and the window size for averaging (1–2 MeV).

The gross structure observed in cosδ must arise from the nonstatistical part of the capture amplitude for *both* $E1$ and $E2$, since the statistical part of either amplitude will not contribute. The observed energy dependence suggests giant resonance phases in both $E1$ and $E2$. In a simple model where we take the average $E1$ and $E2$ amplitudes to be given by single-level Breit-Wigner expressions, we get

$$\delta = \delta_1 + \sigma_1 - \delta_2 - \sigma_2 + \phi_R(1) - \phi_R(2) + \Delta\alpha \ .$$

Here δ_l and σ_l are the nuclear and Coulomb phase shifts for the $l=1$ ($E1$) and $l=2$ ($E2$) entrance channels, and

$$\phi_R(l) = \tan^{-1} 2(E - E_l)/\Gamma$$

is the resonance phase for the $l=1$ (giant $E1$) and $l=2$ (giant $E2$) resonances. The factor $\Delta\alpha$, which we assume constant (independent of energy), includes the mixing phase difference as well as the signs of the electromagnetic matrix elements. To get an idea of the energy variation of the channel phase difference

$$\delta_1 + \sigma_1 - \delta_2 - \sigma_2 \ ,$$

we performed optical model calculations for $\alpha + ^{24}$Mg scattering with $U = -110$ MeV, $W = -4$ MeV, $r_0 = 1.8$ fm, $a = 0.5$ fm, and $r_c = 1.33$ fm. These represent average parameters taken from $\alpha + ^{24}$Mg elastic scattering fits[32] in this energy region. The remarkable result is that this channel phase difference is essentially constant, $175° \pm 3°$ for $E_\alpha = 8$–14 MeV. Below $E_\alpha = 8$ MeV the channel phase difference drops rapidly owing to an $l=2$ shape resonance near 7 MeV. However, this resonance lies outside the range of data fitted,[32] and is likely an artifact of the particular potential parameters chosen. Hence it appears reasonable to neglect the energy dependence in the channel phase difference below $E_\alpha = 8$ MeV as well. From Refs. 33 and

8 we estimate $E_1=20.25$ MeV, $\Gamma_1=4.5$ MeV, $E_2=18.5$ MeV, and $\Gamma_2=6.0$ MeV. The solid curve in Fig. 10 shows cosδ computed from

$$\delta=\phi_R(E1)-\phi_R(E2)+\Delta\alpha$$

with the resonance parameters given above and $\Delta\alpha$ (the only adjustable parameter) set to 116°.

The similarity of the solid and dashed curves in Fig. 10 supports our interpretation of the gross structure in cosδ as being due to gross structure phases (and amplitudes) in both $E1$ and $E2$ channels. The two curves would agree even better if one were to choose somewhat higher resonance energies and somewhat narrower widths. Such gross structure interference effects in cosδ should scale as the product $f_1 \cdot f_2$, where f_l represents the fraction of nonstatistical contributions to the El capture amplitude. It should be emphasized that the solid curve in Fig. 10 is based on the assumption $f_1 \cdot f_2=1$. Hence large f_l are required for a modest gross structure in cosδ. This results from the fact that the GDR and GQR are fairly broad and lie nearly on top of each other.

The existence of such a strong nonstatistical component in the $E2$ channel is not surprising (see the above discussion). However, the $E1$ channel is believed to be (80±20) % statistical (see the fluctuation analysis of σ_{E1} given in Ref. 16), consistent with the view that $\sigma_{E1}(\alpha,\gamma)$ arises mainly from (1) isospin mixing of the GDR with compound 1^-, $T=0$ states; to our knowledge our experiment provides the first evidence for nonstatistical gross structure in an isospin-forbidden giant resonance reaction. A nonstatistical $E1$ component must arise from a different mechanism such as (2) semidirect excitation of the GDR through its isospin-admixed component of the "giant" isoscalar 1^- resonance (the latter being generated by the r^3Y_{1m} operator). Shikazono and Terasawa[27] calculated both of these processes for this reaction—they find that process (1) dominates but that process (2) results in a peak cross section ≈ 1 μb assuming a doorway isospin mixing intensity of 2.25%. Since from experiment $\bar{\sigma}_{E1}\approx 5$—7 μb in the region of the GDR peak, a value of f_1 as large as 0.5 seems plausible due to process (2). Thus it is quite possible that process (2) is sufficiently strong to account for the nonstatistical $E1$ component necessary to produce the observed gross structure in cosδ.

V. SUMMARY

The $^{24}Mg(\alpha,\gamma_0)^{28}Si$ measurements we have presented here are the most detailed experimental results currently available for $E1$ and $E2$ cross sections in an (α,γ) reaction in the giant resonance region. A strongly fragmented $E2$ strength is observed, consistent in magnitude and shape with the results of a ^{28}Si $(\alpha,\alpha'\alpha_0)^{24}Mg$ decay-coincidence experiment. $E1$ cross sections are consistent with roughly 25% compound isospin mixing intensity, as was found previously in neighboring nuclei. Strong $E1$-$E2$ interference effects were observed, due to both a rapidly varying narrow structure and broad gross structure, indicating strong nonstatistical components in both $E1$ and $E2$ channels. The nonstatistical $E2$ component in α_0 may arise from a doorway 1p-1h contribution, as discussed in Ref. 10. The nonstatistical $E1$ component in α_0 is more surprising and may arise from a semidirect amplitude due to doorway isospin mixing. The degree of isospin purity in compound nuclear states is important in HF statistical decay branching ratio estimates.

ACKNOWLEDGMENTS

One of us (E.K.) would like to thank the University of Washington for financial support and the members of the UW Nuclear Physics Laboratory for their kind hospitality. This work was supported in part by the U. S. Department of Energy and in part by the Deutsche Forschungsgemeinschaft.

[1]J. M. Moss, C. M. Rozsa, D. H. Youngblood, J. D. Bronson, and A. D. Bacher, Phys. Rev. Lett. 34, 748 (1975).
[2]K. T. Knöpfle, G. J. Wagner, A. Kiss, M. Rogge, C. Mayer-Böricke, and Th. Bauer, Phys. Lett. 64B, 263 (1976).
[3]K. Van der Borg, M. N. Harakeh, S. Y. Van der Werf, A. Van der Woude, and F. E. Bertrand, Phys. Lett. 67B, 405 (1977).
[4]K. Van der Borg, M. N. Harakeh, and A. Van der Woude, Nucl. Phys. A365, 243 (1981).
[5]K. T. Knöpfle, G. J. Wagner, P. Paul, H. Breuer, C. Mayer-Böricke, M. Rogge, and P. Turek, Phys. Lett. 74B, 191 (1978).
[6]G. J. Wagner, *Giant Multipole Resonances,* edited by F. E. Bertrand (Harwood-Academic, New York, 1980), p. 251.
[7]K. T. Knöpfle, *Lecture Notes in Physics,* No. 108 (Springer, Berlin, 1979), p. 311.

[8]K. T. Knöpfle, H. Riedesel, K. Schindler, G. J. Wagner, C. Mayer-Böricke, W. Oelert, M. Rogge, and P. Turek, Phys. Rev. Lett. 46, 1372 (1981).
[9]D. H. Youngblood, A. D. Bacher, D. R. Brown, J. D. Bronson, J. M. Moss, and C. M. Rozsa, Phys. Rev. C 15, 246 (1977).
[10]K. T. Hecht and D. Braunschweig, Nucl. Phys. A295, 34 (1978).
[11]K. A. Snover, E. G. Adelberger, and D. R. Brown, Phys. Rev. Lett. 32, 1061 (1974).
[12]G. S. Foote, D. Branford, N. Shikazono, and D. C. Weisser, J. Phys. A 7, L27 (1974).
[13]E. Kuhlmann, E. Ventura, J. R. Calarco, D. G. Mavis, and S. S. Hanna, Phys. Rev. C 11, 1525 (1975); E. Kuhlmann, J. R. Calarco, V. K. C. Cheng, D. G. Mavis, J. R. Hall, and S. S. Hanna, *ibid.* 20, 5 (1979).
[14]K. A. Snover, J. E. Bussoletti, K. Ebisawa, T. A. Trainor, and A. B. McDonald, Phys. Rev. Lett. 37, 273 (1976).
[15]L. Meyer-Schützmeister, R. E. Segel, K. Raghunathan, P. T. Debevec, W. R. Wharton, L. L. Rutledge, and T. R. Ophel, Phys. Rev. C 17, 56 (1978).
[16]L. Meyer-Schützmeister, Z. Vager, R. E. Segel, and P. P. Singh, Nucl. Phys. A108, 180 (1968).
[17]R. E. Marrs, E. G. Adelberger, and K. A. Snover, Phys. Rev. C 16, 61 (1977).
[18]L. C. Northcliffe and R. F. Schilling, Nucl. Data Tables A7, 233 (1970).
[19]M. K. Mehta, W. E. Hunt, and R. H. Davis, Phys. Rev. 160, 791 (1967); D. Bodansky and A. Seamster, private communication.
[20]The original value of 14.5% in Table II of Ref. 15 has been rescaled to account for the presently used radius $\langle R^2 \rangle = 9.61$ fm^2 in the $E2$ EWSR.
[21]H. Riedesel, Doctoral thesis, Heidelberg, 1979 (unpublished).
[22]K. A. Snover, *Giant Multipole Resonances,* edited by. F. E. Bertrand (Harwood-Academic, New York, 1980), p. 229.
[23]STAT−2, a Hauser-Feshbach computer code, R. G. Stokstad, Oak Ridge National Laboratory, 1975.
[24]G. F. Perey, Phys. Rev. 131, 745 (1963).
[25]L. McFadden and G. R. Satchler, Nucl. Phys. 84, 177 (1966).
[26]J. R. Huizenga and G. Igo, Nucl. Phys. 29, 462 (1961).
[27]N. Shikazono and T. Terasawa, Nucl. Phys. A250, 260 (1975).
[28]H. L. Harney, H. A. Weidenmüller, and A. Richter, Phys. Rev. C 16, 1774 (1977).
[29]P. P. Singh, R. E. Segel, L. Meyer-Schützmeister, S. S. Hanna, and R. G. Allas, Nucl. Phys. 65, 577 (1965).
[30]J. Ahrens, H. Borchert, K. H. Czock, H. B. Eppler, H. Gimm, H. Gundrum, M. Kröning, P. Riehn, G. Sita Ram, A. Zieger, and B. Ziegler, Nucl. Phys. A251, 479 (1975).
[31]E. Kuhlmann, Phys. Rev. C 20, 415 (1979).
[32]S. S. So, C. Mayer-Böricke, and R. H. Davis, Nucl. Phys. 84, 641 (1964).
[33]B. L. Berman, Nucl. Data Tables 15, 319 (1975).